Title

Repeated monitoring of corneal nerves by confocal microscopy as an index of peripheral neuropathy in type-1 diabetic rodents and the effects of topical insulin

Journal

Journal of the Peripheral Nervous System, 18(4)

ISSN

1085-9489

Authors

Chen, Debbie K
Frizzi, Katie E
Guernsey, Lucie S
et al.

Publication Date

2013-12-01

DOI

10.1111/jns5.12044

Peer reviewed

Published in final edited form as:
J Peripher Nerv Syst. 2013 December ; 18(4): 306–315. doi:10.1111/jns5.12044.

Repeated monitoring of corneal nerves by confocal microscopy as an index of peripheral neuropathy in type-1 diabetic rodents and the effects of topical insulin

Debbie K. Chen, **Katie E. Frizzi**, **Lucie S. Guernsey**, **Kelsey Ladt**, **Andrew P. Mizisin**, and **Nigel A. Calcutt**

Department of Pathology, University of California, San Diego School of Medicine, La Jolla, CA, USA

Abstract

We developed a reliable imaging and quantitative analysis method for *in vivo* corneal confocal microscopy in rodents and used it to determine whether models of type-1 diabetes replicate the depletion of corneal nerves reported in diabetic patients. Quantification was reproducible between observers and stable across repeated time points in two rat strains. Longitudinal studies were performed in normal and streptozotocin-diabetic rats, with innervation of plantar paw skin quantified using standard histological methods after 40 weeks of diabetes. Diabetic rats showed an initial increase, then a gradual reduction in occupancy of nerves in the sub-basal plexus so that values were significantly lower at week 40 (68±6%) than age-matched controls (80±2%). No significant loss of stromal or intra-epidermal nerves was detected. In a separate study, insulin was applied daily to the eye of control and streptozotocin-diabetic mice and this treatment prevented depletion of nerves of the sub-basal plexus. Longitudinal studies are viable in rodents using corneal confocal microscopy and depletion of distal corneal nerves precedes detectable loss of epidermal nerves in the foot, suggesting that diabetic neuropathy is not length dependent. Loss of insulin-derived neurotrophic support may contribute to the pathogenesis of corneal nerve depletion in type 1 diabetes.

Keywords

diabetic neuropathy; distal neuropathy; insulin therapy; in vivo corneal confocal microscopy; streptozotocin; type-1 diabetes

Introduction

Corneal confocal microscopy (CCM) has been widely used to characterize the anatomy of corneal nerves *(Labbe et al., 2006; Esquenazi et al., 2007; Stachs et al., 2007; Mathew et al., 2008; Marfurt et al., 2010)*. The capacity to perform repeated measurements without tissue removal or damage is valuable for monitoring progress after laser in-situ keratomileusis (LASIK) procedures *(Moilanen et al., 2008; Kymionis et al., 2009)* and a variety of conditions such as keratoconus *(Hollingsworth et al., 2005)* and complications of keratosmileusis *(Pisella et al., 2001; Kymionis et al., 2009)*.

Address correspondence to: Debbie K. Chen, Department of Pathology, University of California, San Diego, 9500 Gilman Drive, MC 0612, La Jolla, CA 92093-0612, USA. Tel: 858-822-5797; Fax: 858-534-1886; d3chen@ucsd.edu.

There is growing interest in the use of CCM to measure innervation of the cornea as a non-invasive index of peripheral neuropathies *(Ferrari et al., 2010; Tavakoli et al., 2010b)*, including diabetic neuropathy *(Rosenberg et al., 2000; Chang et al., 2006; Midena et al., 2006; Hertz et al., 2011)*. Changes in corneal nerve morphology are sufficiently sensitive to identify patients with mild neuropathy, as indicated by symptoms, electrophysiology and skin biopsy *(Quattrini et al., 2007)* and to detect efficacy of intervention by pancreatic transplantation *(Mehra et al., 2007;Tavakoli et al. 2013)*. CCM has also been used to study corneal anatomy in assorted animals *(Kafarnik et al., 2007; 2008, Reichard et al., 2010)*. Establishing the presence and natural history of corneal nerve damage in models of diabetes and the relative sensitivity of this technique compared to other widely used indices of diabetic neuropathy may reveal a clinically relevant target for mechanistic and therapeutic preclinical studies and compliment the continuing development of CCM as an index of peripheral neuropathy.

The application of CCM to longitudinal studies of disease progression requires rigorous image collection protocols to obviate observer bias or data variability arising from the marked differences in corneal nerve anatomy at different locations *(Dvorscak and Marfurt, 2008; Patel et al., 2009)*. The purpose of our study was to develop a reproducible method for quantifying corneal nerves of rodents using CCM, to establish the relative sensitivity of corneal nerve density as measured by CCM versus other indices of neuropathy in rodent models of type-1 diabetes and to determine whether corneal nerve depletion in type 1 diabetes is related to insulin deficiency.

Materials and Methods

Animals

All animal protocols were approved by the Institutional Animal Care and Use Committee (IACUC) of University of California, San Diego. In order to assess assay reproducibility and establish any between-strain differences, 9 female albino Sprague-Dawley rats (245-295 g) and 8 age-matched female, pigmented Long-Evans rats (260-289 g) were monitored every 4 weeks for 3 months. Female Sprague-Dawley rats (221-253 g) were then used for a longitudinal study of the impact of type-1 diabetes on corneal nerves while female Swiss Webster mice (25-30 g) were used to assess impact of topical insulin to the eye. Rats were made diabetic with a single dose of streptozotocin (STZ: 55 mg/kg i.p.) *(Calcutt, 2004)*. Mice were made diabetic by injection of STZ (90 mg/kg, i.p.) on two consecutive days *(Davidson et al., 2009)*. Blood glucose levels were measured 4 days after injection of STZ and animals with blood glucose levels of >15 mmol/l were considered diabetic. Age-matched animals served as controls. For insulin treatment, 0.1 IU of regular U-100 Humulin (Lilly, Indianapolis, IN) in 10 μl saline *(Guo et al., 2011)* was applied directly on the eye of 8 control and 8 diabetic mice daily for 4 weeks and corneal nerve occupancy compared to control and diabetic mice receiving saline treatments.

Plasma insulin, blood glucose and HbA1c

Blood was collected from the tail by venipuncture and glucose concentration measured using the OneTouch ultra mini system (LifeScan, Inc., Milipitas, CA, USA). Blood was centrifuged and 50 μl of plasma used to measure insulin concentration by ELISA (Ultrasensitive Rat Insulin kit, Mercodia, Uppsala, Sweden). HbA1c was measured using the A1CNow system (Bayer, Sunnyvale, CA, USA).

Animal imaging platform

A small animal platform (Fig. 1) was developed for use with the Heidelberg Retina Tomograph 3 with Rostock Cornea Module (Heidelberg Engineering, Heidelberg,

Germany). The chin rest was removed and the animal platform placed on the chin rest attachment of the microscope. The imaging platform consists of a base platform supporting two independent moving parts: a) nose cone for the continuous application of isoflurane anesthesia and b) body platform with Velcro straps for body and head restraint. The relative distance between nose cone and body platform can be adjusted for different sized animals. A small attachment to the body platform raises the head for additional adjustment for optimal imaging of the cornea. The base platform can swivel to orientate the animal such that the laser light enters perpendicular to the corneal surface at the apex. The entire platform can be removed, turned 180° and placed back on the chin rest attachment to image both eyes.

Imaging procedures

Under isoflurane (2% in oxygen) anesthesia, rats or mice were placed on the imaging platform and secured with body and head straps such that the eyes were open and one eye was facing the objective of the CCM. GenTeal gel (Novartis Pharmaceuticals Corp., East Hanover, NJ, USA) was placed on both eyes for laser light coupling and to prevent the eye from drying. The microscope objective was positioned to the center apex of the cornea using the laser reflection on the eye and real-time images. By using the objective focus, depth was set to zero at the internal reflection of the tomocap, being careful not to position the objective such that the pressure from the tomocap begins to wrinkle the corneal surface *(Kobayashi et al., 2006)*. The depth was adjusted to 15 μm and one volume stack of 40 images (384× 384 pixels, 1 μm lateral resolution) was collected. Under the volume scan option, the microscope automatically refocuses 10 μm superficial to the set depth and collects volumes up to 80 μm in depth (2 μm depth resolution), resulting in a volume stack from approximately 5-80 μm. Images were collected every 4 weeks and nerve occupancy in the sub-basal plexus and stromal layers of the cornea quantified using a custom designed graphical user interface developed from MATLAB (Natick, MA, USA).

Image analysis and quantification

We defined the progression from sub-basal plexus to stromal layers by the disappearance of the fine, linear corneal nerves of the sub-basal plexus and the highly reflective background along with the appearance of bright keratocytes and large nerve fibers on a dark background *(Labbe et al., 2006)*. Once the sub-basal:stromal junction was determined, inter-animal concordance was achieved using the last image of the sub-basal plexus and the first image of the stroma as fixed anatomical points. Each image was viewed by eye and nerves traced using a WACOM Bamboo tablet (Saitama, Japan) in Image J (NIH) software. Composite images were made by layering all images from sub-basal plexus using Adobe PhotoShop (San Jose, CA), with color-coding of the traces from each image (Fig. 2).

In the absence of continuous images of nerves in the sub-basal plexus, even after stacking in a volume scan, we developed an alternative quantification system based on occupancy. Each image of a volume scan was loaded into MATLAB and a 5×5 grid overlaid for a total of 25 possible occupancies per image. In preliminary modeling studies, we compared 3×3, 5×5, 8×8 and 10×10 grids (data not shown). If a nerve was observed anywhere inside a box, that box was counted as occupied (Fig. 2). For each image, the number of boxes in the grid containing one or more nerves was counted. Nerve occupancy was calculated for both the sub-basal plexus and stromal layers of the cornea. Equation 1 shows the formula for calculating % nerve occupancy per layer, per animal:

$$\%\ \ nerve\ \ occupancy = \left(\frac{total\ \ \#\ \ boxes\ \ occupied\ \ by\ \ nerves\ \ in\ \ layer}{\#\ \ of\ \ images\ \ in\ \ laye^{*}\ \ total\ \ \#\ \ of\ \ boxes\ \ in\ \ grid} \right) * \ 100 \quad \text{(Eq. 1).}$$

Average nerve occupancy was measured at each image depth and then organized by distance from the sub-basal plexus:stromal junction. Volume average analysis was conducted by calculating the average nerve occupancy of the entire volume of sub-basal plexus or stromal layers.

Epidermal nerves

Hind paw skin (plantar surface) was fixed overnight at 4°C in 4% paraformaldehyde in 0.1 M sodium phosphate buffer. The skin was processed, hemisectioned and embedded in paraffin. Sections were cut at a thickness of 6 μm and collected onto glass slides then treated with 3% hydrogen peroxide for 15 minutes followed by normal goat serum (Vectastain Rabbit IgG ABC Kit, Vector Laboratories #PK4001, Burlingame, CA) for 30 minutes. Sections were incubated in a primary antibody against rabbit anti-human Protein Gene Product 9.5 (PGP9.5) (1:1000; AbD Serotec #7863-0504, Raleigh, NC) overnight at 4°C. They were then washed and incubated with biotinylated goat anti-rabbit secondary antibody (Vectastain ABC Kit) for 1 hour, followed by a wash and incubation with an avidin-biotin complex solution (Vectastain ABC Kit) for an additional 1 hour. The reaction product was demonstrated by NovaRed staining (NovaRed Peroxidase Substrate Kit, Vector Laboratories #SK4800). Gill's hematoxylin was used as a counterstain. Skin was viewed using a light microscope and the number of nerve profiles of intra-epidermal nerve fibers (IENFs) and sub-epidermal nerve plexi (SNP) counted and quantified per unit length of the dermal:epidermal junction in the section *(Beiswenger et al., 2008b)*.

Results

Imaging platform performance, image quantification, inter-observer variability and strain dependence

The imaging platform was able to successfully restrain and provide continuous isoflurane anesthesia during image collection with repositioning and re-collecting the images being occasionally necessary. Images (384 × 384 pixels) were collected, with each representing a 400 × 400 μm area of the cornea. Image collection (one volume stack of 40 images) took approximately 2 minutes per animal. Nerves were visible in both the sub-basal region and the stroma but were not continuous, even after tracing and stacking consecutive images (Fig. 2). This prevented accurate measurement of nerve length, density, branching or tortuosity as used in human studies, and prompted us to calculate nerve occupancy as an alternative. Inter-observer variability was studied using 3 independent observers trained according to a standard operating protocol and who counted sub-basal plexus nerve occupancy using volume stacks from 10 Sprague-Dawley rats. Observers were allowed to make the decision to exclude images deemed uncountable because of excessive leukocyte infiltration or brightness of background. There were no significant between-observer differences in measured occupancy (79.5±2.4%, vs 80.1± 3.9% vs 76.6± 4.3%: mean ± SEM). Nerve occupancy in the sub-basal plexus and stroma did not vary within or between rat strains when measured monthly from 23-31 weeks of age by a single observer (Fig. 3).

Corneal and epidermal nerves in long-term diabetic rats

Hyperglycemia was evident 3 days after STZ administration (24.5 ± 1.5 mmol/L) and was sustained (29.0 ± 1.1 mmol/L) compared to controls (5.5 ± 0.1 mmol/L). Body weight, HbA1c and plasma insulin of diabetic rats were all significantly ($p<0.05$, unpaired t-test) different from that of controls at the mid-point (weeks 16 or 24) and end (week 40) of the study, indicating sustained diabetes (Table 1). Nerve occupancy in the sub-basal plexus and stroma of control rats was consistent throughout the study (Fig. 4). Diabetes caused a transient increase in nerve occupancy within the sub-basal plexus during weeks 8-16, that receded to become a significant decrease from week 32 onwards (Fig. 4a). Nerve occupancy

in the stroma was not significantly altered by diabetes (Fig. 4b). There was no significant difference in IENF or SNP values in paw skin between control and diabetic rats at week 40 (Fig. 5).

Corneal nerves in diabetic mice and effects of topical insulin

STZ-treated mice showed significant hyperglycemia (30.6 ± 1.2 mmol/L) compared to controls (8.6 ± 0.5 mmol/L: $p<0.001$). Delivery of insulin (0.1-1.0 IU) to the eye did not acutely alter blood glucose levels of control or diabetic mice (Fig. 6A). Topical insulin treatment to the eye (0.1 IU daily) for 4 weeks did not change nerve occupancy in the sub-basal plexus of control mice (saline: 28.9 ± 1.7%, insulin: 29.0 ± 2.9%: Fig. 6B). Diabetic mice receiving saline treatment showed a significant decrease in nerve occupancy in the sub-basal plexus (22.2 ± 3.5, $p<0.05$) compared to control animals and this was prevented in insulin treated diabetic mice (29.0 ± 1.7%).

Discussion

We successfully adapted the Heidelberg HRT corneal confocal microscope for use in rats and mice. Images were collected from the entire volume stack of 80 μm depth from the epithelial layer to the anterior stroma. The epithelial layer contained hexagonal cells with dark borders and bright cytoplasm in the superficial epithelium and bright borders and dark cytoplasm in the basal epithelium *(Guthoff et al., 2006)*. The appearance of small, linearly directed nerve fibers traversing a bright, reflective background lacking epithelial cells or keratocytes indicated the sub-basal nerve plexus immediately above Bowman's layer. Two studies reported an absence of Bowman's layer in rats *(Jakus, 1954; Davson, 1984)*. However, recent technical advances have increased resolution and we routinely detected nerves across 4-5 consecutive images in healthy rats and mice. Mice exhibited lower nerve occupancy than rats in this region, which may reflect detection limits of the finer nerves in mice. Progression to the anterior stroma was indicated by emergence of keratocytes and large, highly reflective and randomly directed stromal nerves on a dark background. This transition was used as an anatomic reference point for aligning volume stack data from individual animals into a group analysis.

Nerves of the sub-basal plexus have the typical linear appearance noted in prior qualitative studies *(Labbe et al., 2006; Esquenazi et al., 2007)*. However, unlike published images from humans using this particular corneal confocal microscope *(Efron et al., 2010)*, nerves in the sub-basal plexus were not continuous but moved in and out of plane of section. Stacking consecutive images did not provide a complete view of individual nerves, presumably because these fine nerves cannot be resolved when in the plane between adjacent images, 2 μm apart. This prevented accurate use of measures such as nerve length, branching or tortuosity that are commonly used in clinical studies *(Quattrini et al., 2007; Tavakoli et al., 2010b)*. We therefore developed a method in which the apical corneal volume from the corneal epithelia through to the anterior stroma was sampled in 2 μm sections to obviate image selection bias and then applied a simple yes/no grid occupancy system to allow rapid quantitative analysis of nerve fragments. This is analogous to the profile counting technique used to quantify terminal branches of IENF in skin biopsies *(Beiswenger et al., 2008b)*. Another novel feature of our analysis is the collection and quantification of serial, rather than random or selected images. Most human studies collect and assay representative images rather than all layers of the volume stack. In order to test our training and operating procedures, three observers were trained to count images and produced data that agreed closely. The advantages of the occupancy system applied across all images of a volume stack include an unbiased image collection method and the ease of use and reproducibility of the yes/no quantification method. Sensitivity of the method is related to the size of the grid.

Smaller grid sizes increase sensitivity but can also increase difficulty in making accurate decisions due to the fixed magnification of the CCM. Careful consideration of sensitivity requirements should therefore be considered for each study.

We first demonstrated the stability of iterative measurements of nerve occupancy by collecting images from the cornea of two rat strains at monthly intervals for 3 months. Previous studies have demonstrated strain differences in retinopathy *(Dorfman et al., 2009; Kirwin et al., 2009; Kern et al., 2010)* and there are deficiencies in the visual acuity of albino rats compared to pigmented rats *(Grant et al., 2001; Prusky et al., 2002)*. We found no differences between healthy pigmented and non-pigmented rats at any point across the 12-week study period. Our results also show that calculating nerve occupancy from CCM images can provide reliable iterative measurements in rodents.

One application of quantitative and iterative CCM in rodents is to allow evaluation of their pertinence as models of chronic neurodegenerative disease. Changes in corneal nerve architecture detected by CCM have been proposed as biomarkers of peripheral neuropathy in diabetic patients *(Quattrini et al., 2007)*. We therefore performed a longitudinal study of corneal nerve occupancy in a rat model of type 1 diabetes. Nerve occupancy was initially increased in the sub-basal plexus after 8 and 16 weeks of diabetes while nerve occupancy in the stromal layer was unchanged, suggesting a phenomenon specific to distal regions of the axon. Increased nerve occupancy could arise from either increased nerve tortuosity, as reported in some patients showing impaired glucose tolerance *(Tavakoli et al., 2010b)*, or collateral sprouting. While we are not aware of prior reports using CCM in type 1 diabetic rats that could guide our interpretation of this increase in occupancy, there is precedence in other sensory nerve terminals, as type 1 diabetes caused an early and transient increase in density of IENF in foot pad skin of mice *(Beiswenger et al., 2008a)*. This increase in nerve density was accompanied by an increase in the number of axons expressing Growth Associated Protein (GAP) 43, a marker of growing or regenerating axons. The presence of GAP-43 in epidermal sensory nerve terminals of normal rodents *(Beiswenger et al., 2008a; Cheng et al., 2010)* and humans (Fantini and Johansson, 1992; Bursova et al., 2012) has been interpreted as evidence for continuous terminal plasticity and remodeling. Whether corneal sensory nerves share this apparently dynamic phenotype remains to be established.

Continued monitoring of corneal nerves demonstrated that the initial increase in occupancy in the sub-basal plexus of diabetic rats eventually progressed to a sustained decrease in occupancy. This is consistent with reports of reduced corneal nerve length in cross sectional clinical studies using CCM in type 1 diabetic patients *(Quattrini et al., 2007; Pritchard et al., 2011; Tavakoli et al., 2011b)* and a rat model of type-2 diabetes *(Davidson et al., 2012a)*. The progression from increased to decreased corneal nerve occupancy also has precedence in the increase, then eventual decrease, in IENF density seen in paw skin from STZ-diabetic mice *(Beiswenger et al., 2008a)*, although the rate of progression was much faster in the mice. The slower progression in the present study could reflect differences in species, nerve location or the underlying pathogenic mechanism. However, it should also be noted that the present cohort showed a relatively mild degree of diabetes as they did not lose weight over time and had detectable residual plasma insulin levels. STZ-induced diabetes is occasionally criticized for the severity of insulinopenia and rapid onset of nerve dysfunction compared to human type 1 diabetes. We have fortuitously studied a physiologically stable cohort of diabetic rats that highlights the pertinence of corneal nerve depletion as an index of early neuropathy and its potential as a tool for evaluating efficacy of potential therapeutic agents in an assay that replicates a clinical condition.

Nerve occupancy remained normal in the stroma of diabetic rats suggesting a distal axonopathy, as indicated by other measures of diabetic polyneuropathy *(Sima et al., 1983;*

Fernandez et al., 2012; Hoke, 2012), including a recent histological evaluation of corneal innervation in 8-week STZ-diabetic rats that showed depletion of nerves in the epithelium before any effect on the sub-basal plexus *(Davidson et al., 2012b)*. In the present study, the decrease in the nerves of the sub-basal plexus occurred in the absence of any detectable loss in paw skin IENF measurements from the same animals. Our assay is sensitive enough to detect IENF loss after 4 weeks in severely STZ-diabetic mice *(Beiswenger et al., 2008a)* and after 20 weeks in other STZ-diabetic rats *(Roy Chowdhury et al., 2012)*. The absence of IENF depletion in the present cohort of STZ-diabetic rats emphasizes their mild neuropathy phenotype. It also suggests that corneal nerve occupancy provides a particularly sensitive marker of neuropathy and argues against the concept that susceptibility to distal neuropathy is confined to long nerves. Similar interpretations can be drawn from clinical studies in which reduced corneal nerve length was as sensitive as IENF depletion as a marker of mild diabetic neuropathy *(Quattrini et al., 2007; Tavakoli et al., 2010a)*.

Reduced occupancy in the sub-basal nerve plexus of type 1 diabetic rodents could feasibly arise from hyperglycemia, dyslipidemia or other downstream consequences of impaired insulin signaling. Depletion of neurotrophic support has been frequently implicated in the pathogenesis of diabetic neuropathy and NGF deficient mice have reduced corneal innervation *(de Castro et al., 1998)*. Our finding that topical delivery of insulin to the eye of diabetic mice prevented reduced nerve occupancy in the sub-basal plexus, without any effects on systemic glycemic control, suggests that insulinopenia *per se* may contribute or that local insulin can compensate for other lesions. There is emerging interest in the role of deficient insulin signaling arising from either reduced insulin production or receptor dysfunction in the pathogenesis of diabetic neuropathy, independent of glucose modulation. Insulin serves as a growth factor for peripheral sensory nerves *(Fernyhough et al., 1993; Xu et al., 2004; Toth et al., 2006)*, preserves mitochondrial function in sensory nerves from diabetic rats *(Huang et al., 2003)* and protects against assorted indices of neuropathy *(Singhal et al., 1997; Huang et al., 2003; Brussee et al., 2004; Hoybergs and Meert. 2007; Jolivalt et al., 2008; Romanovsky et al., 2010)*, including IENF depletion *(Toth et al., 2006; Guo et al., 2011)*. Interestingly, the environment surrounding distal corneal nerves is similar to that of sensory nerves in the epidermis, in that both regions rely in part on oxygen diffusion from the exterior and nerves receive support from local cells via diverse factors including neurotrophin family members, CNTF, BDNF and IGF-1 *(Muller et al., 2003; Calcutt et al., 2008)*. Whether depletion of corneal nerves during long-term diabetes shares the same pathogenesis as other regions of the PNS remains to be investigated.

This study has shown that volume-scanning CCM with quantification of nerve occupancy can be used to continuously monitor nerves in a long-term disease such as diabetes. The technique is robust and can detect time-dependent increases and subsequent decreases in nerve occupancy. STZ-diabetic rodents model the nerve damage reported in the cornea of diabetic patients and may be useful for investigating the pathogenesis of neuropathy and evaluation of potential therapeutic interventions to restore established neuropathy by systemic or topical delivery.

Acknowledgments

The authors thank Natalie Nelson, Maria Rodriguez and Kevin Van Smaalen for technical assistance. The authors thank the NIH (AMDCC grant DK076169, sub-award 23789-5 to NAC) and the JDRF (postdoctoral fellowship # 3-2011-349 to DKC) for funding.

References

Beiswenger KK, Calcutt NA, Mizisin AP. Dissociation of thermal hypoalgesia and epidermal denervation in streptozotocin-diabetic mice. Neurosci Lett. 2008a; 442:267–272. [PubMed: 18619518]

Beiswenger KK, Calcutt NA, Mizisin AP. Epidermal nerve fiber quantification in the assessment of diabetic neuropathy. Acta Histochem. 2008b; 110:351–362. [PubMed: 18384843]

Brussee V, Cunningham FA, Zochodne DW. Direct insulin signaling of neurons reverses diabetic neuropathy. Diabetes. 2004; 53:1824–1830. [PubMed: 15220207]

Bursova S, Dubovy P, Vlckova-Moravcova E, Nemec M, Klusakova I, Belobradkova J, Bednarik J. Expression of growth-associated protein 43 in the skin nerve fibers of patients with type 2 diabetes mellitus. J Neurol Sci. 2012; 315:60–63. [PubMed: 22209024]

Calcutt NA, Jolivalt CG, Fernyhough P. Growth factors as therapeutics for diabetic neuropathy. Current Drug Targets. 2008; 9:47–59. [PubMed: 18220712]

Calcutt NA. Modeling diabetic sensory neuropathy in rats. Methods Mol Med. 2004; 99:55–65. [PubMed: 15131329]

Chang PY, Carrel H, Huang JS, Wang IJ, Hou YC, Chen WL, Wang JY, Hu FR. Decreased density of corneal basal epithelium and subbasal corneal nerve bundle changes in patients with diabetic retinopathy. Am J Ophthalmol. 2006; 142:488–490. [PubMed: 16935596]

Cheng C, Guo GF, Martinez JA, Singh V, Zochodne DW. Dynamic plasticity of axons within a cutaneous milieu. J Neurosci. 2010; 30:14735–14744. [PubMed: 21048132]

Davidson E, Coppey L, Lu B, Arballo V, Calcutt NA, Gerard C, Yorek M. The roles of streptozotocin neurotoxicity and neutral endopeptidase in murine experimental diabetic neuropathy. Exp Diabetes Res. 2009; 2009:431980. [PubMed: 20148083]

Davidson EP, Coppey LJ, Holmes A, Yorek MA. Changes in corneal innervation and sensitivity and acetylcholine-mediated vascular relaxation of the posterior ciliary artery in a type 2 diabetic rat. Invest Ophthalmol Vis Sci. 2012a; 53:1182–1187. [PubMed: 22273725]

Davidson EP, Coppey LJ, Yorek MA. Early loss of innervation of cornea epithelium in streptozotocin-induced type 1 diabetic rats: improvement with ilepatril treatment. Invest Ophthalmol Vis Sci. 2012b; 53:8067–8074. [PubMed: 23169880]

Davson H. The Eye. 1984; 1B:12–26.

de Castro F, Silos-Santiago I, Lopez de Armentia M, Barbacid M, Belmonte C. Corneal innervation and sensitivity to noxious stimuli in trkA knockout mice. Eur J Neurosci. 1998; 10:146–152. [PubMed: 9753121]

Dorfman AL, Polosa A, Joly S, Chemtob S, Lachapelle P. Functional and structural changes resulting from strain differences in the rat model of oxygen-induced retinopathy. Invest Ophthalmol Vis Sci. 2009; 50:2436–2450. [PubMed: 19168901]

Dvorscak L, Marfurt CF. Age-related changes in rat corneal epithelial nerve density. Invest Ophthalmol Vis Sci. 2008; 49:910–916. [PubMed: 18326711]

Efron N, Edwards K, Roper N, Pritchard N, Sampson GP, Shahidi Am, Vagenas D, Russell A, Graham J, Dabbah MA, Malik RA. Repeatability of measuring corneal subbasal nerve fiber length in individuals with type 2 diabetes. Eye Contact Lens. 2010; 36:245–248. [PubMed: 20724854]

Esquenazi S, He J, Li N, Bazan NG, Esquenazi I, Bazan HE. Comparative in vivo high-resolution confocal microscopy of corneal epithelium, sub-basal nerves and stromal cells in mice with and without dry eye after photorefractive keratectomy. Clin Experiment Ophthalmol. 2007; 35:545–549. [PubMed: 17760637]

Fantini F, Johansson O. Expression of growth-associated protein 43 and nerve growth factor receptor in human skin: a comparative immunohistochemical investigation. J Invest Dermatol. 1992; 99:734–742. [PubMed: 1281863]

Fernandez DC, Pasquini LA, Dorfman D, Aldana Marcos HJ, Rosenstein RE. Early distal axonopathy of the visual pathway in experimental diabetes. Am J Pathol. 2012; 180:303–313. [PubMed: 22079928]

Fernyhough P, Willars GB, Lindsay RM, Tomlinson DR. Insulin and insulin-like growth factor I enhance regeneration in cultured adult rat sensory neurones. Brain Res. 1993; 607:117–124. [PubMed: 8481790]

Ferrari G, Gemignani F, Macaluso C. Chemotherapy-associated peripheral sensory neuropathy assessed using in vivo corneal confocal microscopy. Arch Neurol. 2010; 67:364–365. [PubMed: 20212239]

Grant S, Patel NN, Philp AR, Grey CN, Lucas RD, Foster RG, Bowmaker JK, Jeffery G. Rod photopigment deficits in albinos are specific to mammals and arise during retinal development. Vis Neurosci. 2001; 18:245–251. [PubMed: 11417799]

Guo G, Kan M, Martinez JA, Zochodne DW. Local insulin and the rapid regrowth of diabetic epidermal axons. Neurobiol Dis. 2011; 43:414–421. [PubMed: 21530660]

Guthoff RF, Baudouin C, Stave J. Atlas of Confocal Laser Scanning In-vivo Microscopy in Ophthalmology. Springer, Berlin. 2006

Hertz P, Bril V, Orszag A, Ahmed A, Ng E, Nwe P, Ngo M, Perkins BA. Reproducibility of in vivo corneal confocal microscopy as a novel screening test for early diabetic sensorimotor polyneuropathy. Diabet Med. 2011; 28:1253–1260. [PubMed: 21434993]

Hoke A. Animal models of peripheral neuropathies. Neurotherapeutics. 2012; 9:262–269. [PubMed: 22415319]

Hollingsworth JG, Efron N, Tullo AB. In vivo corneal confocal microscopy in keratoconus. Ophthalmic Physiol Opt. 2005; 25:254–260. [PubMed: 15854073]

Hoybergs YM, Meert TF. The effect of low-dose insulin on mechanical sensitivity and allodynia in type I diabetes neuropathy. Neurosci Lett. 2007; 417:149–154. [PubMed: 17412508]

Huang TJ, Price SA, Chilton L, Calcutt NA, Tomlinson DR, Verkhratsky A, Fernyhough P. Insulin prevents depolarization of the mitochondrial inner membrane in sensory neurons of type 1 diabetic rats in the presence of sustained hyperglycemia. Diabetes. 2003; 52:2129–2136. [PubMed: 12882932]

Jakus MA. Studies on the cornea. I. The fine structure of the rat cornea. Am J Ophthalmol. 1954; 38:40–53.

Jolivalt CG, Lee CA, Beiswenger KK, Smith JL, Orlov M, Torrance MA, Masliah E. Defective insulin signaling pathway and increased glycogen synthase kinase-3 activity in the brain of diabetic mice: parallels with Alzheimer's disease and correction by insulin. J Neurosci Res. 2008; 86:3265–3274. [PubMed: 18627032]

Kafarnik C, Fritsche J, Reese S. Corneal innervation in mesocephalic and brachycephalic dogs and cats: assessment using in vivo confocal microscopy. Vet Ophthalmol. 2008; 11:363–367. [PubMed: 19046276]

Kafarnik C, Fritsche J, Reese S. In vivo confocal microscopy in the normal corneas of cats, dogs and birds. Vet Ophthalmol. 2007; 10:222–230. [PubMed: 17565554]

Kern TS, Miller CM, Tang J, Du Y, Ball SL, Berti-Matera L. Comparison of three strains of diabetic rats with respect to the rate at which retinopathy and tactile allodynia develop. Mol Vis. 2010; 16:1629–1639. [PubMed: 20806092]

Kirwin SJ, Kanaly ST, Linke NA, Edelman JL. Strain-dependent increases in retinal inflammatory proteins and photoreceptor FGF-2 expression in streptozotocin-induced diabetic rats. Invest Ophthalmol Vis Sci. 2009; 50:5396–5404. [PubMed: 19474406]

Kobayashi A, Yokogawa H, Sugiyama K. In vivo laser confocal microscopy of Bowman's layer of the cornea. Ophthalmology. 2006; 113:2203–2208. [PubMed: 17157133]

Kymionis GD, Diakonis VF, Kalyvianaki M, Portaliou D, Siganos C, Kozobolis VP, Pallikaris AI. One-year follow-up of corneal confocal microscopy after corneal cross-linking in patients with post laser in situ keratosmileusis ectasia and keratoconus. Am J Ophthalmol. 2009; 147:774–778. [PubMed: 19200532]

Labbe A, Liang H, Martin C, Brignole-Baudouin F, Warnet JM, Baudouin C. Comparative anatomy of laboratory animal corneas with a new-generation high-resolution in vivo confocal microscope. Curr Eye Res. 2006; 31:501–509. [PubMed: 16769609]

Marfurt CF, Cox J, Deek S, Dvorscak L. Anatomy of the human corneal innervation. Exp Eye Res. 2010; 90:478–492. [PubMed: 20036654]

Mathew JH, Bergmanson JP, Doughty MJ. Fine structure of the interface between the anterior limiting lamina and the anterior stromal fibrils of the human cornea. Invest Ophthalmol Vis Sci. 2008; 49:3914–3918. [PubMed: 18765633]

Mehra S, Tavakoli M, Kallinikos PA, Efron N, Boulton AJ, Augustine T, Malik RA. Corneal confocal microscopy detects early nerve regeneration after pancreas transplantation in patients with type 1 diabetes. Diabetes Care. 2007; 30:2608–2612. [PubMed: 17623821]

Midena E, Brugin E, Ghirlando A, Sommavilla M, Avogaro A. Corneal diabetic neuropathy: a confocal microscopy study. J Refract Surg. 2006; 22:S1047–S1052. [PubMed: 17444092]

Moilanen JA, Holopainen JM, Vesaluoma MH, Tervo TM. Corneal recovery after lasik for high myopia: a 2-year prospective confocal microscopic study. Br J Ophthalmol. 2008; 92:1397–1402. [PubMed: 18650214]

Muller LJ, Marfurt CF, Kruse F, Tervo TM. Corneal nerves: structure, contents and function. Exp Eye Res. 2003; 76:521–542. [PubMed: 12697417]

Patel DV, Tavakoli M, Craig JP, Efron N, McGhee CN. Corneal sensitivity and slit scanning in vivo confocal microscopy of the subbasal nerve plexus of the normal central and peripheral human cornea. Cornea. 2009; 28:735–740. [PubMed: 19574916]

Pisella P, Auzerie O, Bokobza Y, Debbasch C, Baudouin C. Evaluation of corneal stromal changes in vivo after laser in situ keratomileusis with confocal microscopy. Ophthalmology. 2001; 108:1744–1750. [PubMed: 11581044]

Pritchard N, Edwards K, Shahidi AM, Sampson GP, Russell AW, Malik RA, Efron N. Corneal markers of diabetic neuropathy. Ocul Surf. 2011; 9:17–28. [PubMed: 21338566]

Prusky GT, Harker KT, Douglas RM, Whishaw IQ. Variation in visual acuity within pigmented, and between pigmented and albino rat strains. Behav Brain Res. 2002; 136:339–348. [PubMed: 12429395]

Quattrini C, Tavakoli M, Jeziorska M, Kallinikos P, Tesfaye S, Finnigan J, Marshall A, Boulton AJ, Efron N, Malik RA. Surrogate markers of small fiber damage in human diabetic neuropathy. Diabetes. 2007; 56:2148–2154. [PubMed: 17513704]

Reichard M, Hovakimyan M, Wree A, Meyer-Lindenberg A, Nolte I, Junghans C, Guthoff R, Stachs O. Comparative in vivo confocal microscopical study of the cornea anatomy of different laboratory animals. Curr Eye Res. 2010; 35:1072–1080. [PubMed: 20961216]

Romanovsky D, Wang J, Al-Chaer ED, Stimers JR, Dobretsov M. Comparison of metabolic and neuropathy profiles of rats with streptozotocin-induced overt and moderate insulinopenia. Neuroscience. 2010; 170:337–347. [PubMed: 20600635]

Rosenberg ME, Tervo TM, Immonen IJ, Muller LJ, Gronhagen-Riska C, Vesaluoma MH. Corneal structure and sensitivity in type 1 diabetes mellitus. Invest Ophthalmol Vis Sci. 2000; 41:2915–2921. [PubMed: 10967045]

Roy Chowdhury SK, Smith DR, Saleh A, Schapansky J, Marquez A, Gomes S, Akude E, Morrow D, Calcutt NA, Fernyhough P. Impaired adenosine monophosphate-activated protein kinase signalling in dorsal root ganglia neurons is linked to mitochondrial dysfunction and peripheral neuropathy in diabetes. Brain. 2012; 135:1751–1766. [PubMed: 22561641]

Sima AA, Bouchier M, Christensen H. Axonal atrophy in sensory nerves of the diabetic BB-Wistar rat: a possible early correlate of human diabetic neuropathy. Ann Neurol. 1983; 13:264–272. [PubMed: 6847138]

Singhal A, Cheng C, Sun H, Zochodne DW. Near nerve local insulin prevents conduction slowing in experimental diabetes. Brain Res. 1997; 763:209–214. [PubMed: 9296561]

Stachs O, Zhivov A, Kraak R, Stave J, Guthoff R. In vivo three-dimensional confocal laser scanning microscopy of the epithelial nerve structure in the human cornea. Graefes Arch Clin Exp Ophthalmol. 2007; 245:569–575. [PubMed: 16941142]

Tavakoli M, Kallinikos P, Iqbal A, Herbert A, Fadavi H, Efron N, Boulton AJ, Malik R. Corneal confocal microscopy detects improvement in corneal nerve morphology with an improvement in risk factors for diabetic neuropathy. Diabet Med. 2011b; 28:1261–1267. [PubMed: 21699561]

Tavakoli M, Quattrini C, Abbott C, Kallinikos P, Marshall A, Finnigan J, Morgan P, Efron N, Boulton AJ, Malik RA. Corneal confocal microscopy: a novel noninvasive test to diagnose and stratify the

severity of human diabetic neuropathy. Diabetes Care. 2010a; 33:1792–1797. [PubMed: 20435796]

Tavakoli M, Marshall A, Pitceathly R, Fadavi H, Gow D, Roberts ME, Efron N, Boulton AJ, Malik A. Corneal confocal microscopy: A novel means to detect nerve fibre damage in idiopathic small fibre neuropathy. Exp Neurol. 2010b; 223:245–250. [PubMed: 19748505]

Tavakoli M, Mitu-Pretorian M, Petropolous IN, Fadavi H, Asghar O, Alam U, Ponirakis G, Jeziorska M, Marshall A, Efron N, Boulton AJ, Augustine T, Malik RA. Early nerve regeneration in diabetic neuropathy after simultaneous pancreas and kidney transplantation. Diabetes. 2013; 62:254–260. [PubMed: 23002037]

Toth C, Brussee V, Martinez JA, McDonald D, Cunningham FA, Zochodne DW. Rescue and regeneration of injured peripheral nerve axons by intrathecal insulin. Neuroscience. 2006; 139:429–449. [PubMed: 16529870]

Xu Q, Li X, Kotecha SA, Cheng C, Sun HS, Zochodne DW. Insulin as an in vivo growth factor. Exp Neurol. 2004; 188:43–51. [PubMed: 15191801]

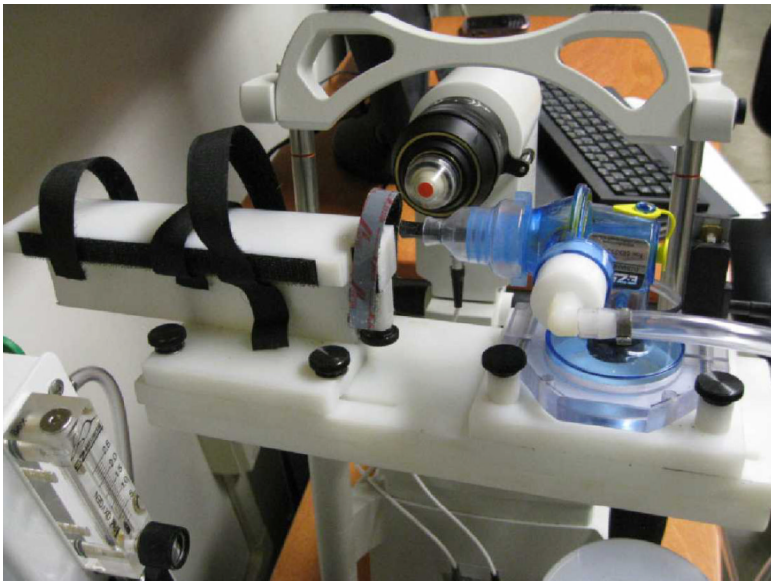

Figure 1.
Custom animal imaging platform developed for use in conjunction with the Heidelberg Retina Tomograph 3 with Rostock Cornea Module.

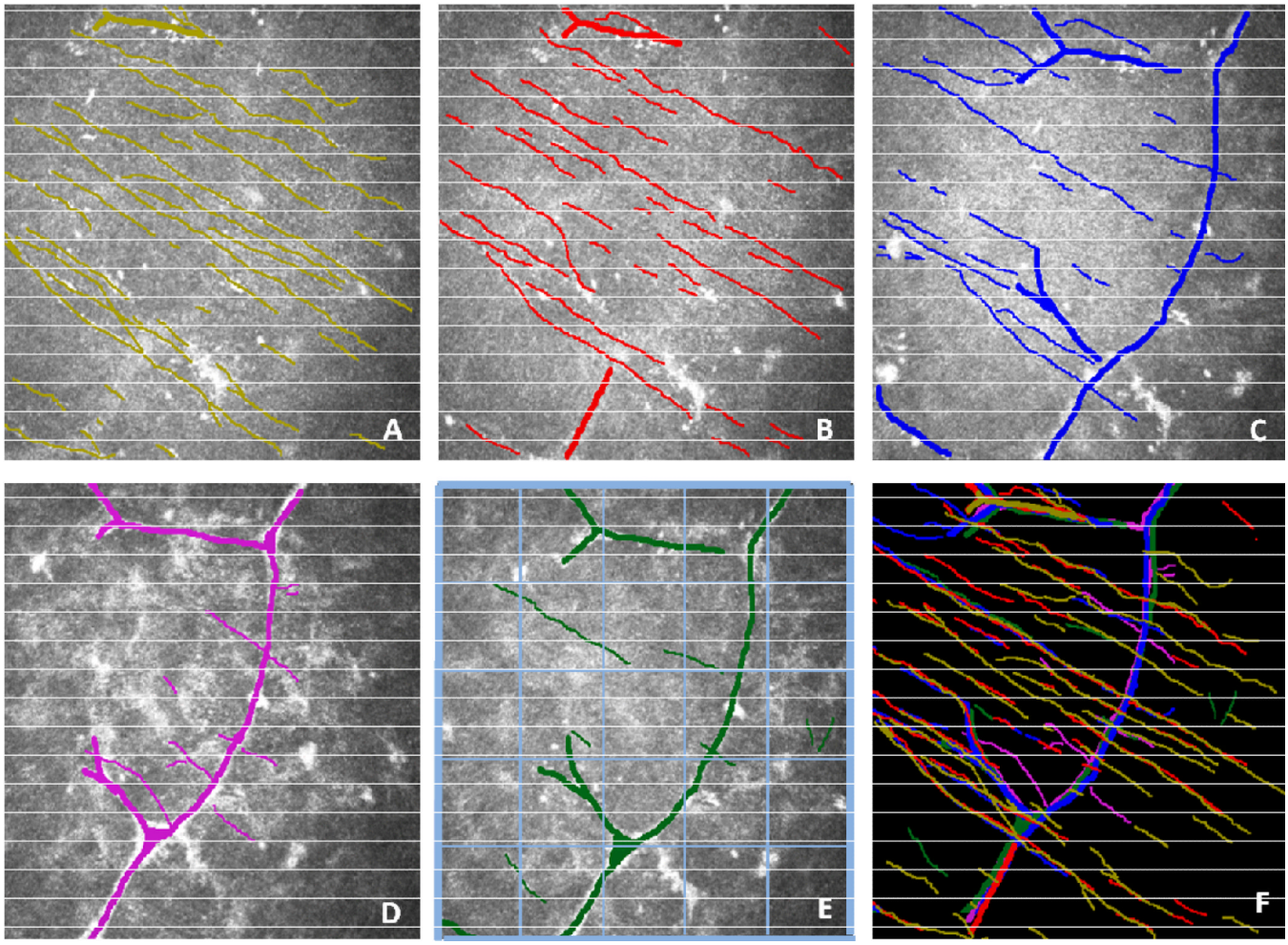

Figure 2.

A sequence of images, 2 μm apart, spanning the sub-basal nerve plexus. Visible sub-basal (thin colored lines) and stromal (thick colored lines) nerves are traced in each layer (A-E). A representative 5×5 grid is overlaid on image E to demonstrate quantification of nerve occupancy. The composite tracing of 5 layers is shown in (F), with each layer shown in a different color.

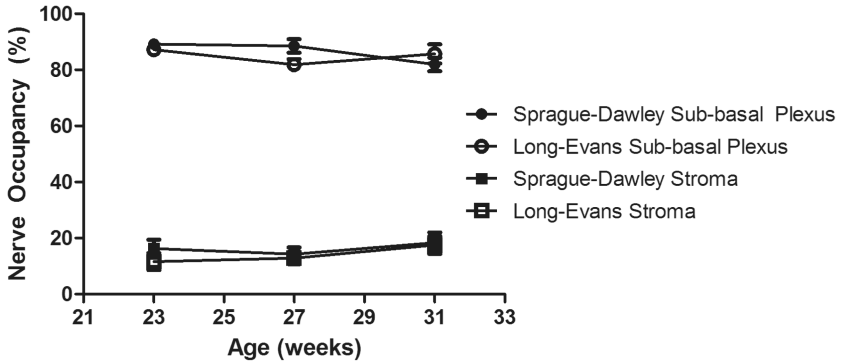

Figure 3.

Nerve occupancy (%) in the sub-basal plexus and stroma of Sprague-Dawley (N=9) and Long-Evans (N=8) rats. Data points represent group mean ± SEM.

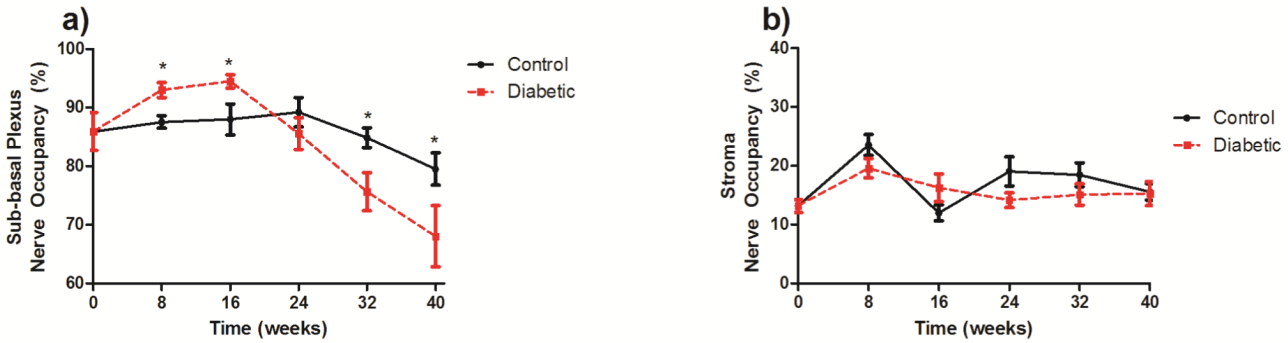

Figure 4.

Volume averaged nerve occupancy (%) of the sub-basal plexus (a) and the stroma (b). Data are group mean ± SEM. In the sub-basal plexus, 2-way ANOVA indicates that groups are significantly different ($p<0.05$), time course is significantly different ($p<0.001$) and the interaction is significantly different ($p<0.01$).

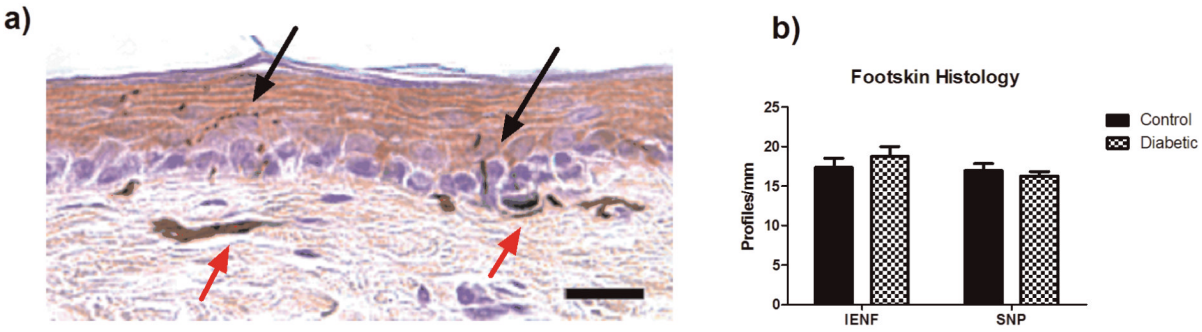

Figure 5.

a) A representative image of foot skin where black arrows indicate IENF and red arrows indicate SNP. b) Quantification of IENF profiles/mm at week 40. Data are group mean ± SEM. Bar = 20 μm.

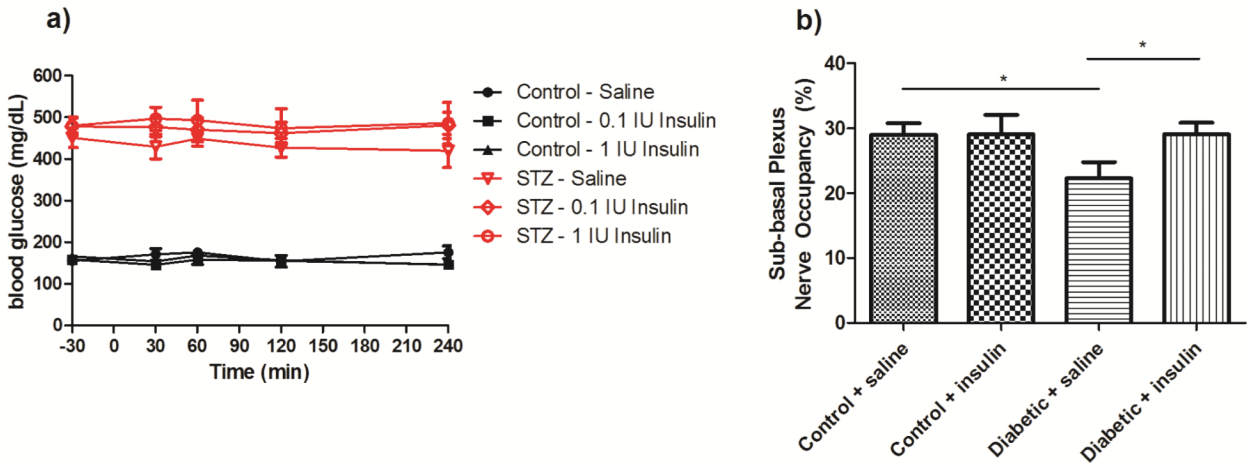

Figure 6.

Effect of topical insulin delivery to the eye on systemic blood glucose levels (a) and of chronic insulin delivery on nerve occupancy in the sub-basal plexus after 4 weeks of diabetes (b). N=8 per group. Data are group mean ± SEM. *p<0.05 by ANOVA with Student Newman Keuls post-hoc test.

Table 1

Physiological parameters during diabetes in streptozotocin-injected rats.

	Onset		Mid-point		End-point	
	Control (n=10)	**Diabetic (n=10)**	**Control (n=10)**	**Diabetic (n=10)**	**Control (n=10)**	**Diabetic (n=8)**
weight (g)	234 ± 2	235 ± 2	294 ± 3	257 ± 9**	316 ± 3	262 ± 15**
HbA1c (%)	--	--	4.2 ± 0.1	10.2 ± 0.4***	4.2 ± 0.1	9.3 ± 0.9***
plasma insulin (μg/l)	--	--	0.73 ± 0.17	0.23 ± 0.1***	0.78 ± 0.11	0.11 ± 0.04*

Body weight and plasma insulin were measured at weeks 16 and 40, while HbA1c was measured at weeks 24 and 40. Data are group mean±SEM. Unpaired t-test was used to test significance,

* =p<0.05,

** =p<0.01,

*** =p<0.001.